In unison: First- and second-order information combine for integration of shape information

Ken W. S. Tan The University of Western Australia, School of Psychology, Crawley, WA, Australia

J. Edwin Dickinson The University of Western Australia, School of Psychology, Crawley, WA, Australia

David R. Badcock The University of Western Australia, School of Psychology, Crawley, WA, Australia

The modulation of orientation around radial frequency (RF) patterns and RF textures is globally processed in both cases. This psychophysical study investigates whether the combination—a textured RF path obtained by applying an RF texture to an RF contour—is processed like a texture or a contour when making judgements about shape. Unlike RF textures, the impression of a closed flow was not required for global integration of textured RF paths, suggesting that these paths were processed as second-order, or contrast-defined contours. Luminance-defined (LD) RF paths were shown to globally integrate but with thresholds approximately half of those for the proposed second-order textured paths. The next experiment investigated whether this benefit was due to LD stimuli possessing double the amount of information (first- and second-order information). A mixed three-part contour composed of two different second-order texture components and an LD component was then employed to determine how the different cues combined. The mixed path thresholds matched predictions derived from a linear combination of first- and second-order cues. The conclusion is that the shape of isolated contours is processed using both first- and second-order information equally and that the contribution of texture is to carry additional second-order signal.

Introduction

The ability to interact appropriately with objects in the environment requires the observer to recognize the specific target objects. One way we do this is by being able to visually distinguish the shape of the target from other nontarget shapes. Being able to determine the shape of an object is therefore a critical step in object recognition and this often entails delineating the two-dimensional extent, or boundary, of an object. The position of a boundary in noise can be determined in numerous ways. If the boundary is defined by a contrast in luminance then this process can begin with the visual system detecting local elements of oriented luminance information and combining them to form the bounding contour (Loffler, 2008; Wilson & Wilkinson, 2015). Salience of such a boundary in noise is enhanced by means of early stages of visual processing highlighting and facilitating the detection of contour fragments that continue smoothly across a visual scene (Field, Hayes, & Hess, 1993; Kapadia, Westheimer, & Gilbert, 2000; Li & Gilbert, 2002) and human functional magnetic resonance imaging (fMRI) studies have revealed stronger responses to contours containing collinear elements than randomly oriented elements (Altmann, Bülthoff, & Kourtzi, 2003). Although there is some evidence that familiar contours are more salient than unfamiliar (Nygård, Sassi, & Wagemans, 2011), the process described above is often termed *contour extraction* as it involves delineating the boundary rather than analysis of the shape of the boundary. It is assumed in this study that it is once the boundary has been extracted from its context that analysis of the shape of the object is then possible. The enhancement of the salience of collinear elements has been modeled as being due to excitatory long range lateral connections between neurons with similar orientation preference (Field et al., 1993). As well as accounting for the enhanced salience of collinear paths, this mechanism can also explain the salience in noise of smooth paths of Gabor patches consistently aligned perpendicular to the path (Bex, Simmers, & Dakin,

Citation: Tan, K. W. S., Dickinson, J. E., & Badcock, D. R. (2016). In unison: First- and second-order information combine for integration of shape information. *Journal of Vision, 16*(11):9, 1–14, doi:10.1167/16.11.9.

doi: 10.1167/16.11.9 Received July 10, 2015; published September 12, 2016 ISSN 1534-7362

2001; Ledgeway, Hess, & Geisler, 2005; Marotti, Pavan, & Cascoa, 2012). Such paths do not provide a luminance cue at the boundary, but if the gain of the neurons responsible for the detection of the elements of the path is enhanced relative to a background then such a path might become visible because of exaggerated sensitivity to the luminance-contrast properties of the boundary. Once a path is rendered visible against its context then analysis of the shape of the path can proceed. Marotti et al. (2012) framed this observation in terms of Gestalt principles of grouping. Both paths composed of collinear patches (snakes) and parallel patches (ladders), are enhanced in salience when presented in noise due to their similarity in orientation, but the salience of collinear paths are also enhanced by good continuation. Significantly, Marotti et al. (2012) reported that the salience of a ladder was enhanced slightly if the phases of the patches were randomized. They argued that this might be due to a reduction in inhibitory crowding interactions between parallel elements when the contrast difference between adjacent elements was randomized and concluded that the salience of snakes and ladders was mediated by a balance between excitatory and inhibitory lateral interactions at an early level of analysis in the visual system. Under such a system, the salience of a path would depend upon a complex of lateral interactions, although it is probable that the excitatory lateral interactions of collinear elements would predominate. In a recent study, Wilder, Feldman, and Singh (2016) used information theoretic arguments to model contour detection in noise as a decision problem. Observers were required to report, in a two-interval forced choice task, the interval that contained a path. It was found that as complexity of the path increased, the ability to detect the path decreased. In their model, complexity is a strong function of the curvature of the path, but the distribution of the complexity on the path was shown to be unimportant. This indicates that observers were not performing the task by searching for straight-line segments and suggests that the salience of the path in noise must be considered holistically. Reconciliation of this information theoretic model with the association field model (Field et al., 1993) will, however, require more work. For our purposes, although we recognize that shape inevitably influences the salience of paths in noise, we suggest that the analysis of the shape of the path occurs after it is detected.

In this study, we use paths of Gabor patches that are aligned tangential to the path, perpendicular to the path, and at random to the path. The paths are presented in isolation in the sense that no noise patches are presented as context to the path. The paths are, therefore, always visible. We use a forced choice task to ascertain the amount of deformation of a circular path that is necessary to reliably discriminate a deformed path from a circular path. The data obtained therefore describes the capacity for discriminating two shapes rather than detecting a path within noise.

One stimulus that has been particularly useful in the study of the discrimination of shape is the radial frequency (RF) pattern. RF patterns are contours produced by sinusoidally modulating the radius of a circle (Wilkinson, Wilson, & Habak, 1998) and have frequently been used to demonstrate the global integration of modulation information in contours (Dickinson, Han, Bell, & Badcock, 2010; Loffler, Wilson, & Wilkinson, 2003; Schmidtmann, Kennedy, Orbach, & Loffler, 2012; Tan, Dickinson, & Badcock, 2013). As more cycles of modulation (CoMs) are added to an RF pattern of a particular frequency, thresholds for discriminating between the modulated RF pattern and an unmodulated pattern (i.e., a circle) decrease. This could potentially be attributed to probability summation (PS) of near threshold signals. PS here is defined as the increasing probability of detecting local deformation from circularity as more CoMs are progressively introduced. However, what is generally observed is that thresholds decrease at a rate significantly greater than that predicted by PS, and global integration of local modulation information is invoked as the rationale for this superior performance. Depending on the experimental circumstance, there can be varying formulations for the calculation of PS, which can result in different predictions (Kingdom, Baldwin, & Schmidtmann, 2015; Meese & Summers, 2012; Nachmias, 1981; Tyler & Chen, 2000). In order to facilitate comparison with previous studies, we have continued to use the conventional manner in which the PS prediction has been calculated in RF pattern studies (e.g., Dickinson, Cribb, Riddell, & Badcock, 2015; Dickinson et al., 2010; Loffler et al., 2003; Tan, Bowden, Dickinson, & Badcock, 2015; Tan et al., 2013). If PS is assumed, the modulation amplitude thresholds for discrimination of a modulated pattern from a circle are predicted to decline with number of CoMs according to a power function with an index equal to the negative reciprocal of Q, a fitted parameter in the Quick function (Equation 3) as originally outlined by Wilson (1980). The parameter Q describes the slope of the psychometric function relating the probability of correct discrimination to the amplitude of modulation of a stimulus with a particular frequency and number of CoMs. However, the implications of more recently discussed methods for estimating PS will also be addressed in the General discussion.

There has been debate as to when and how global integration is invoked in RF patterns. Schmidtmann et al. (2012) suggested that discrimination thresholds fall at the rate of PS for an incomplete RF pattern (one

with fewer cycles than is required to complete 360°) and only drops below PS predictions once the entirety of the RF pattern is modulated (which necessarily suggests a template model; see also Loffler, 2015), while others (Bell & Badcock, 2008; Dickinson et al., 2015; Dickinson, McGinty, Webster, & Badcock, 2012; Loffler et al., 2003; Tan et al., 2015; Tan et al., 2013) have reported a rapid decrease that is smooth and conforms tightly to a power function with increasing numbers of cycles until the pattern is complete. The improvement in thresholds for low frequency RF patterns exceeds that predicted by PS, indicating global integration, and has led to the proposition of specialized processes that exist in the visual system for shape detection that rely on the analysis of the periodicity of curvature (Kempgens, Loffler, & Orbach, 2013; Poirier & Wilson, 2006). This conclusion is supported by work showing that different frequency RF patterns can be identified at the same threshold required to detect shape modulation (Dickinson, Bell, & Badcock, 2013; Dickinson et al., 2015).

It has been recently demonstrated that like RF patterns, textures comprised of elements that are periodically modulated can also be globally processed (Tan et al., 2015). These textures were created by introducing a RF modulation of orientation to the elements as a function of polar angle, but where the positions of the patches were jittered radially such that the texture contained no contiguous paths (RF texture). As CoMs increased on the RF texture, thresholds for the detection of modulation were observed to fall at a rate that exceeded PS, suggesting global processing of information inherent to the texture. When, however, a texture was used where the orientations of the elements were locally orthogonal to that of an RF texture (RFO texture), no global integration was observed. Such a texture had orientation modulation information present but did not have the subjective impression of closure. This led Tan et al. (2015) to propose that "flowsure" (flowing into closure) appeared to be critical for global integration of orientation modulation in textures.

It must be emphasized that the integration of modulation information in the analysis of shape from texture differs from integration of signal over area as has been demonstrated for Glass patterns (Burr & Ross, 2006; Dickinson, Broderick, & Badcock, 2009). In Glass patterns, signal elements—conventionally dot pairs—have a coherent orientation across the pattern. The position of such signal elements is assigned at random and, therefore, cannot define the polar positions of shape-relevant curvature features. The signal in Glass patterns serves to define a texture, albeit a texture that can have a center, as is the case for concentric and radial Glass patterns. Translational Glass patterns have a texture that is continuous in space and is defined by the orientation of the signal dot pairs relative to the Cartesian plane. Similarly, Motoyoshi and Kingdom (2010) have shown that the configuration of pairs of local oriented elements has a dramatic effect on the perception of a continuous texture. In particular, the visual system was shown to be most sensitive to signal pairs of oriented local stimuli that were co-circular when presented among noise pairs that were oriented at random relative to one another. This preference for co-circularity might be seen as a manifestation of the principle of good continuation in path detection. A similar argument for the accentuation of local path continuity was made by Tversky, Geisler, and Perry (2004), emphasizing the likelihood that local elements belong to the same path. Motoyoshi and Kingdom (2010) also remarked, however, that sensitivity to co-circular elements could be demonstrated as extending into a range of small orientation difference between elements that could not be accounted for using good continuation arguments. They concluded that this sensitivity amounted to detectors for angle. In the study by Tan et al. (2015) the reference stimuli to which modulation was added were equivalent to concentric and radial Glass patterns (with oriented Gabor patches taking the place of dot pairs). In the signal stimuli, the orientations of the local patches were modulated from these reference stimuli as a sinusoidal function of polar angle as though they were component parts of an RF path. Locally, then, pairs of Gabor patches were close to parallel but not usually collinear. Such pairing could not be co-circular and, therefore, could not form paths through the principle of good continuation. Pairs of patches with greater separation though would be co-circular and the angles described by the pairs would vary systematically around the pattern.

In that study (Tan et al., 2015), the threshold amplitude of modulation from concentric was seen to fall steeply as the number of CoMs was increased, indicating that the modulation information was being integrated around the pattern. In contrast, modulation from radial was not integrated around that pattern. This result illustrates an important distinction between the integration along a path of similarly oriented Gabor patches and integration of shape information in RF textures. Continuous paths composed of patches that are approximately collinear or approximately parallel are salient within noise, whereas integration of modulation of orientation is only found for textures with patches modulated from concentric. This result provides the opportunity to examine the interaction of orientation modulation along and perpendicular to a path in the determination of shape.

In this study, then, stimuli that incorporate aspects of both RF contour patterns and modulated textures

are used to examine how the processing of the two might interact. Specifically we ask whether when a modulated texture is applied to an RF contour, does the resultant textured contour adhere to the requirements for integration of orientation modulation in an RF texture (i.e., require flowsure) or does a filter → rectify → filter processing sequence on the luminance information in the local patches allow for a contrast defined, second-order, processing of the orientation modulation of the RF contour. Given that a second-order path exists in the RF patterns with a texture orthogonal to the path, we are essentially asking how the texture information might have an impact on the combination of the luminance-defined (LD) first-order and contrast-defined second-order information intrinsic to RF patterns. To this end we use RF patterns where the orientation of the texture on the path is either aligned tangential to the path, perpendicular to the path, or at random orientations to the path.

General methods

Participants

Two authors and two experienced observers (who were naive to experimental aims) participated in the study. Informed consent was obtained prior to commencement and all participation was voluntary. Observers possessed normal or corrected-to-normal visual acuity. One of the authors has a divergent squint (with normal acuity in both eyes) and completed all experiments monocularly by covering one eye with an opaque eye patch; all other participants used binocular viewing. The treatment of participants in this study complied with the guidelines set by the Human Research Ethics Committee of the University of Western Australia and was in accordance with the tenets of the Declaration of Helsinki.

Apparatus

The custom stimuli used in the experiments were generated using Matlab 7.0.4 (Mathworks, Natick, MA). The program was run on an Intel® Pentium® 4 CPU 3.0 GHz (1024MB RAM) and drawn on a 256 MB frame buffer of a Cambridge Research Systems (CRS) ViSaGe graphics system (CRS, Kent, UK). Stimuli were presented on a Sony Trinitron Multiscan G520 Monitor (resolution: 1024 × 768 [34.13° × 25.6°], refresh rate: 100 Hz, Sony, Tokyo, Japan) at a viewing distance of 65.5 cm. Each square pixel on the screen subtended 2′ of visual angle at this viewing distance and distance was held constant by means of a chinrest. A darkened room (ambient luminance <1cd/m^2) was used as the testing venue. An Optical OP 200-E photometer (Head model #265) and associated software (CRS) was used to calibrate screen luminance. The background luminance to all stimuli was set at 45 cd/m^2. Observer responses were recorded using a CRS CB6 response box.

Stimuli

Four different conditions were run across the two experiments, each is described in their respective experiments. Stimuli were in all cases sampled paths of RF contours composed of 36 Gabor patches (LD sinusoidal gratings localized by a Gaussian contrast window) with gratings that had a carrier spatial frequency of 6 c/°. The Gaussian envelope had a $\sigma =$ 0.067°. The diameter of the envelope of each Gabor path at half maximum contrast was 0.157° and the Michelson contrast was 0.84. The carrier grating of the Gabor was in negative sine phase relative to the center of the envelope, ensuring that the midpoint of the Gabor patch was therefore at background luminance and contrast to background was symmetrical.

Equation 1 defines the radius of the RF contour used in the experiment:

$$R(\theta) = R_0\Big(1 + A\sin(\omega\theta + \varphi)\Big) \quad (1)$$

where $R(\theta)$ is the radius of the pattern at an angle of θ relative to the positive x-axis; R_0 is the base radius (and is in all cases 4° of visual angle); A is the amplitude of distortion from a circle expressed as a proportion of R_0; ω is the frequency of modulation (RF number); and φ is the phase of the modulation (φ was randomized for all stimuli used in this experiment on each trial) Reference stimuli were created using $A = 0$.

Depending on the experiment, patches were aligned tangential to (RF path: Experiment 1A), perpendicular to (RFO path: Experiment 1A), random with respect to (Rand path: Experiment 1B) the contour given by Equation 1, or a combination of these (Mix path: Experiment 2). RF modulated sections and circular sections were smoothed together by fitting a first derivative of a Gaussian (D1) to the transitional part of the sinusoidal contour modulation (Loffler et al., 2003). The D1 had the same maximum amplitude and gradient as the sinusoidal modulation it replaced. RF3 patterns were used throughout the study as they allow the three manipulations of the path in the study to be equally represented on whole CoMs in a complete pattern, and also because they have previously been shown to exhibit integration of information around the pattern that is close to linear (an index of −1 in the power function, Equation 4; Tan et al., 2015).

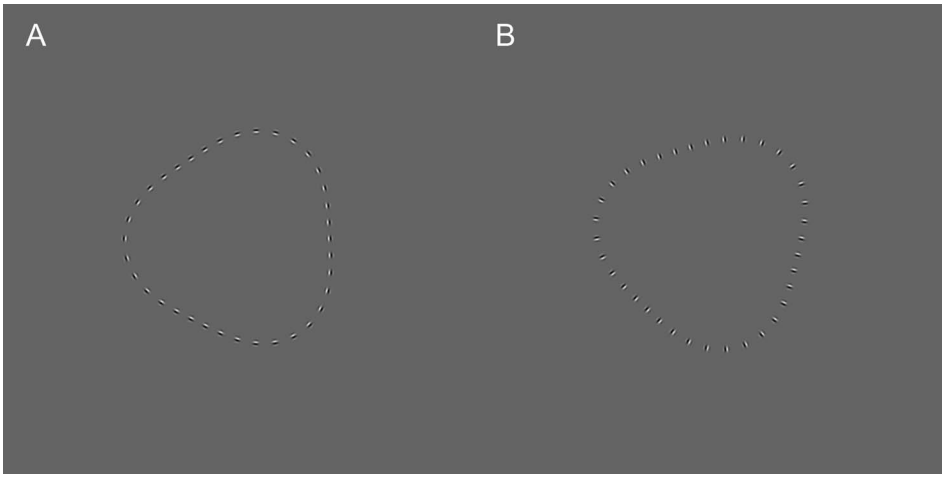

Figure 1. Examples of stimuli used in Experiment 1A. (A) RF path—a conventional sampled RF pattern where the orientation of the elements that comprise the path are tangential to the RF contour. (B) RFO path—similar to the RF path but where the orientation of each element comprising the path has had 90° added to them and the orientation of the patches are perpendicular to the RF contour. Stimuli are presented above threshold for illustration purposes.

Procedure

In a two-interval forced choice task, participants were tasked to indicate the pattern they determined to be the most deformed from circularity. Patterns were presented sequentially and appeared on screen for 160 ms with an interstimulus interval of 500 ms. The test stimulus was an RF pattern that had one, two, or three CoMs with a radial frequency of three cycles per 2π radians (subsequently referred to as RF3 modulation), when the pattern had one or two CoMs, the remainder of the contour was circular. The reference stimulus was in all instances circular. The method of constant stimuli was used to control stimulus presentation with nine different levels of amplitude modulation (A in Equation 1). Stimuli were presented 60 times at each of the nine levels per CoM for each condition, collected across three runs (1,620 trials per condition). Stimuli were presented in separate blocks for CoM and condition.

Experiment 1A

Introduction

It has been previously shown that a continuous RF contour (Bell & Badcock, 2008; Dickinson et al., 2015; Loffler et al., 2003) and sampled RF contour (Dickinson et al., 2010; Tan et al., 2013) can support global integration of shape, as can a modulated texture that appears to have a closed continuous flow, albeit without containing continuous contours (Tan et al., 2015). However, when the modulated texture does not have element orientations that give the impression of flowing into closure (e.g., the RFO texture with elements orthogonal to circular flow), global pooling of the modulated texture does not occur (Tan et al., 2015). This experiment examines how contour and texture cues interact in defining a contour. Does an RFO texture applied to a sampled path (essentially creating a second-order sampled contour) prevent global integration of the contour shape? Two different stimuli were used, one where the orientation of the elements was tangent to the path (RF path, to be used for comparison), and another where the elements were perpendicular to the local tangent to the path (RFO path), thus ensuring that the elements used contained modulation information but that the direction of elements themselves did not lie end to end such that they gave the impression of closure (RFO path; see Figure 1B).

Stimuli

Two different conditions were run in this part of the experiment: RF path and RFO path (see Figure 1 for example stimuli).

For the contour, an angle α was formed between the perpendicular of the patches and the radius. This orientation α is given by:

$$\alpha(\theta) = \tan^{-1}\left(\frac{A\omega\cos(\omega\theta+\varphi)}{R(\theta)/R_0}\right) \quad (2)$$

For the RFO path, $\pi/2$ radians (90°) were added to the α given by Equation 2.

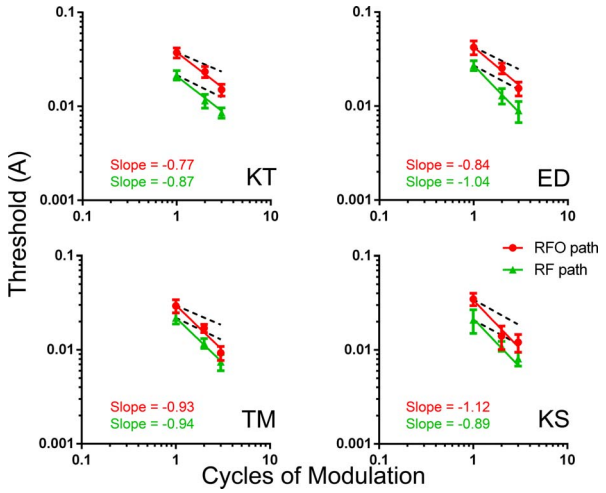

Figure 2. Thresholds for all four observers versus the number of CoMs plotted on logarithmic axes so that the power function index equates to slope (with 95% CIs). Dashed lines represent the respective PS predictions. In all instances observed slopes were steeper than their PS prediction. Slope values for each individual are presented in the font colours that correspond to the respective stimuli.

Results

The proportion of correct responses for the nine test amplitudes was calculated for each condition. A Quick (1974) function (see Equation 3) was fitted to the psychometric data to determine discrimination thresholds:

$$p(A) = 1 - 2^{-\left(1+(A/\Delta)^{Q}\right)} \quad (3)$$

where $p(A)$ is the probability of a correct response for amplitude A; Δ is the threshold in A for discrimination of the test from reference pattern at a 75% correct performance level; and Q is a measure of the slope of the psychometric function (Quick, 1974; Wilson, 1980).

The thresholds for each participant were measured for $n = 1$, 2, and 3 CoMs on the patterns. Δ decreases with the number of CoMs at a rate conforming to a power function:

$$\Delta(n) = Kn^{-\gamma} \quad (4)$$

where γ is the magnitude of the index of the power function and K is a parameter that represents the fitted value of threshold for a single CoM.

For each of the experimental conditions, Δ was plotted against CoM on logarithmic axes to render γ visible as a slope of a straight line (see Figure 2). The estimated magnitude of the index of the power function γ predicted by PS is the reciprocal of the variable Q in the Quick function (Loffler et al., 2003; Quick, 1974; Wilson, 1980). A rate of decrease in threshold greater than that predicted by PS is used as an indicator of global integration of signal across cycles.

As can be seen in Figure 2, slopes of the fits (for all observers) are steeper than their respective PS predictions: RFO path, $t(3) = 8.07$, $p = 0.004$, $R^2 = 0.96$, and RF path, $t(3) = 12.1$, $p = 0.001$, $R^2 = 0.98$.

Discussion

This experiment set out to determine whether a modulated textured contour would be treated as a texture or a contour for global integration of shape. RF textures are textures that are globally integrated. Orienting texture elements orthogonally to the local orientation in RF textures prevents integration (i.e., flowsure is needed to achieve global pooling). We replicated previous findings that demonstrate global pooling of a conventional sampled RF pattern (Dickinson et al., 2010; Tan et al., 2013). The results also show that an RF pattern created by using Gabor patches that were orthogonal to the direction of modulation is globally processed. While there have been studies that have used similar looking stimuli in masking experiments (Habak, Wilkinson, & Wilson, 2009; Habak, Wilkinson, Zakher, & Wilson, 2004), they have generally assumed that continuous RF contours comprised of alternating black and white bars aligned orthogonally to the RF contour were globally processed; to the best of our knowledge this is the first instance explicitly demonstrating RFO paths are globally processed. This finding indicates that unlike the RFO textures used by Tan et al. (2015), flowsure of elements on a contour is not critical for global integration to occur in contours. This also seems to be consistent with the findings of studies suggesting that Glass textures and RF patterns are processed by different detectors (Badcock, Almeida, & Dickinson, 2013; Tan et al., 2015).

Thresholds were observed to be higher for the RFO path than for the RF path; one explanation for this might be that the RF path, being an LD contour, might contain more cues. The RFO path could be thought of as a textured contour or a second-order contour. The premise was that on its own, an RFO texture was not globally processed because it lacked flowsure. When this texture was applied to a contour, the texture itself would not be expected to be globally processed. However, there has also been research using contrast modulated texture to define RF patterns that show global integration can occur with second-order RF patterns (Bell & Badcock, 2008). A filter → rectify → filter model is usually proposed to explain the perception of a second-order stimulus (Graham & Sutter, 1996; Wilson, Ferrera, & Yo, 1992). In the RFO

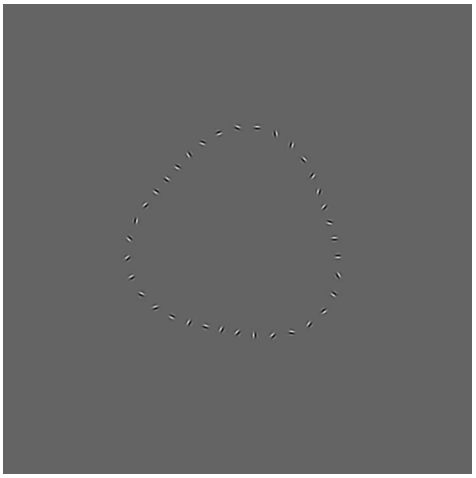

Figure 3. Example of the stimuli (Rand path) used in Experiment 1B. Gabor patches are placed with their centers on the boundary of an RF contour, but have random orientations with respect to the polar angle. The above example is presented above threshold for illustration purposes.

path, the patches always have a luminance contrast relative to the background; however, because the carrier grating is orthogonal to the path, it does not get processed as an LD contour. However, the contrast envelopes do map out a smooth contour, and perhaps the visual system can then use the rectified contrast information from the envelope to support global integration of that path.

The suggestion that the second-order properties of the paths support global integration is consistent with our results. However, even in the RFO path there is systematic variation in element orientation and that modulation could be contributing, even though it does not when using modulated textures. The only way to confirm this is by removing any coherent orientation modulation signal from the applied texture. We proceed to do this in Experiment 1B.

Experiment 1B

Introduction

In this experiment, the aim was to investigate whether the orientation modulation information available in the texture was crucial for integration of a second-order RF contour. This was done by removing the coherent orientation modulation information that was previously in the RFO path and replacing that with patches of random orientation.

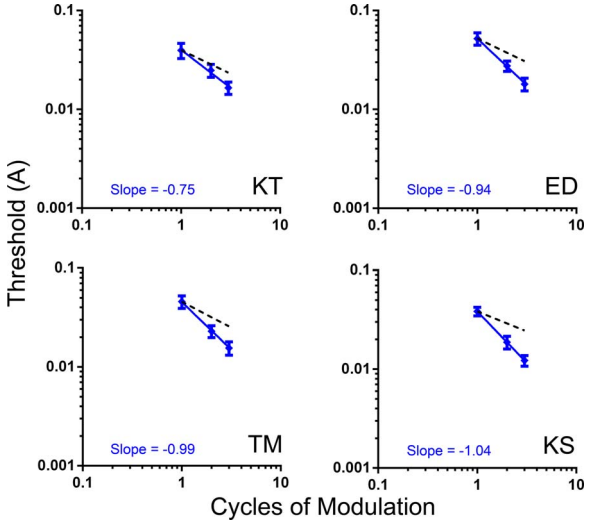

Figure 4. Thresholds of all four observers versus the number of CoMs plotted on logarithmic axes so that the power function index equates to slope (with 95% CIs) for the Rand path stimuli. Dashed lines represent the respective PS predictions. All fits were observed to be steeper than their respective PS.

Stimuli

A path of randomly oriented Gabor patches (Rand path) was the stimulus used in this part of the experiment. Stimulus creation was the same as that described in the General methods with the exception that, α previously defined by Equation 2 was randomly generated for each element (see Figure 3 for example).

Results

As with Experiment 1A, a Quick (1974) function was fitted to the psychometric data and the resultant thresholds were observed to obey a power function when plotted against CoM (see Figure 4).

As shown in Figure 4, fits for all observers were observed to be steeper than their respective PS prediction when slopes were compared to PS predictions with a paired-samples t test, $t(3) = 6.10$, $p = 0.009$, $R^2 = 0.93$. When compared with the results obtained from Experiment 1A, on visual inspection of the data (see Figure 5), with the exception of participant TM, thresholds for the RFO path did not appear to look any different from those for Rand path. A 2×3 (Condition $\times$ CoM) analysis of variance (ANOVA) was consistent with this interpretation as no main effect of Condition, $F(1, 3) = 7.53$, $p = 0.07$, and no interaction effect between the Condition and CoM was observed, $F(2, 6) = 3.75$, $p = 0.09$. CoM did show a main effect, $F(2, 6) = 169.1$, $p < 0.0001$. As a group, a paired-samples t test also showed that slopes for RFO path (M $= -0.91$, 95% CI [-1.15, -0.68]) and Rand path (M =

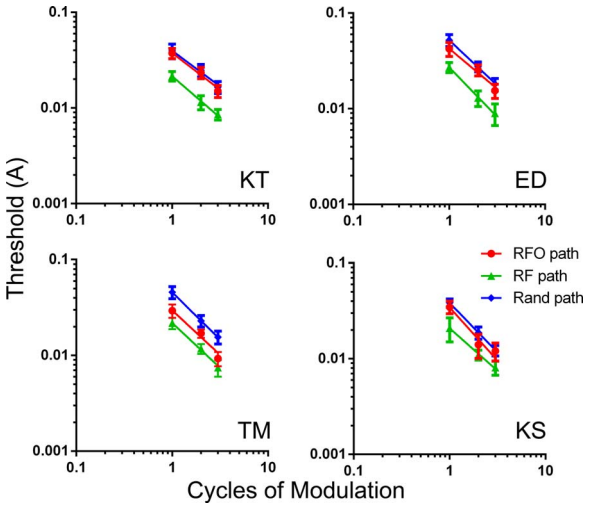

Figure 5. Thresholds for stimuli employed in Experiment 1A and 1B plotted on the same graph for all participants with 95% CIs. As a group, RFO path was not observed to be different from Rand path.

–0.93, 95% CI [–1.13, –0.73]) did not differ from one other, $t(3) = 0.39$, $p = 0.72$, $R^2 = 0.95$.

Discussion

This experiment set out to investigate whether removing the systematic orientation modulation in the applied texture would affect global integration of a textured (second-order) contour. Our results show that despite not having systematic orientation modulation of its component elements, Rand path had threshold improvements that exceeded PS predictions generated using the method introduced by Loffler et al. (2003), suggesting global processing. This again indicated that the pooling of information that was occurring was post-rectification, which allowed a filter oriented along the path to determine the orientation of the envelope. The finding that the thresholds and slopes for the RFO path and the Rand path were not statistically different from one another indicates that the texture orientation modulation present in the RFO path does not have a substantial impact.

Comparing thresholds for the RF path (an LD path) and the two textured paths (RFO path and Rand path; second-order paths), shows that the thresholds for the LD path were systematically lower (approximately half) those for the second-order. One possibility is that the performance benefit might have resulted from the RF path having both first- and second-order cues, while the RFO path and Rand path only had second-order cues, suggesting that perhaps the visual system was capitalizing on the presence of an additional cue. This possibility was investigated in Experiment 2.

Experiment 2

Introduction

In Experiment 1A and 1B, it was observed that contours defined by luminance and second-order (contrast) cues could be globally processed. In addition, it was found that thresholds for these second-order contours were approximately double those for LD contours. LD stimuli, restricted in space, necessarily contain first- and second-order information (Edwards & Badcock, 1995), a luminance variation, and a contrast variation, while a second-order stimulus is designed to only have systematic variation in contrast. The question was whether the performance benefit observed for the RF path (over RFO path and Rand path) was due to the alignment of the first-order cue information, or to the presence of additional first-order cues. The assumption was made that each CoM could only carry one "piece" of first-order information and one "piece" of second-order information as cues (i.e., maximum two cues per CoM). Following this argument, in a second-order contour (e.g., Rand path) the number of second-order cues would increase at the same rate as the number of CoMs. In an LD contour (e.g., RF path) the number of cues (first- and second-order) would increase at double the rate as the number of CoMs increases (i.e., CoM increase from one to three, number of cues increase from two to six). To depict this assumption, the data can be plotted against the number of cues rather than the number of CoMs and, assuming these items of information are being integrated, they should all fall on the same power function, without a vertical offset separating RF Path and Rand Path threshold estimates. Rand path was picked as the second-order contour of choice across the four observers since we can be confident that there is no systematic element-orientation contribution to the processing of that contour. This amalgamation was plotted and the fit revealed steep slopes with strong goodness of fit values ($r^2 = 0.99$; see Figure 6), suggesting that this assumption was plausible.

The plots in Figure 6 show that as the number of cues increases, the threshold fell at a rate steep enough to indicate global pooling. However, this prediction, based on combining the thresholds for two separate LD and second-order contours, needs an independent test. The question was whether this assumption would hold when LD and second-order cues were presented on the same contour in separate segments. Three possibilities arise: (a) only the second-order information will be pooled (since these were common to all CoMs), (b) both first- and second-order information will be pooled with equal weight, or, (c) a probabilistic benefit may arise from having independent detection of both first-

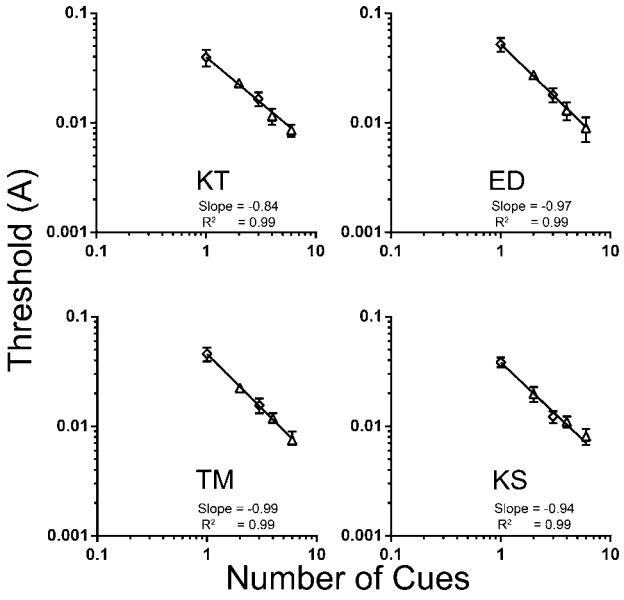

Figure 6. Combined Fit—graphs plotting the thresholds for RF path and Rand path against number of cues on logarithmic axes with 95% CIs for each participant. Slope and goodness of fit of the Combined Fit is presented below each plot. The thresholds from the Rand path are indicated by the diamonds, while the thresholds from the RF path are indicated by the triangles. The threshold of the point at cues = 2 is an average of RF path and Rand path.

and second-order information. To this end, a stimulus (Mix path) was created, comprised of both LD and second-order cues that appear separately on different segments of the contour. As in Experiment 1A and 1B, an RF3 was used. The first CoM was always Rand path so that the orientation of the patches for that section was random, the second cycle was RFO path with the orientation of the patches perpendicular to the RF contour, and the third cycle was RF path (i.e., first and second cycles were second-order, third cycle was first- and second-order) where the orientation of the patches were in accordance with the direction of modulation. The manner in which integration occurred as first- and second- order cues were combined was then investigated. For the first two cycles on the Mix stimulus, the number of cues would increase from one to two. For the third cycle, the data could match one of several possibilities: (a) if only second-order information was used, then thresholds for the third cycle would be consistent with three cues on Figure 6, (b) if both first- and second-order information was used then thresholds would be consistent with four cues, and finally (c) if first- and second-order were used probabilistically then thresholds would be consistent with $\sqrt{10}$ cues (this is the resultant of two orthogonal vectors with magnitudes 3 and 1, which might be expected at the third cycle where there could be three possible instances of second-order information or one possible instance of first-order information, so the magnitude of the resultant vector would be the square root of the sum of the squares of the magnitudes of the first two vectors, $\sqrt{3^2 + 1^2} = \sqrt{10}$).

Stimuli

Creation of the RF contour was similar to that described in the General methods. The stimuli (Mix path) used in this experiment always had the first cycle of RF modulation as Rand path, the second cycle was RFO path, and the final cycle was RF path (see Figure 7). Reference stimuli were circles comprised of all three types.

Results

As before, the psychometric data was fitted with a Quick (1974) function. Thresholds for the third cycle on the Mix stimulus were compared against the predicted Combined Fit shown in Figure 6. Predicted thresholds for three, $\sqrt{10}$, and four cues were derived from the fit of Equation 4 to the combined data in Figure 6. Third cycle thresholds were observed to be statistically different from the three cues prediction, $t(3) = 4.64$, $p = 0.02$, $R^2 = 0.88$, and $\sqrt{10}$ cues prediction, $t(3) = 3.45$, $p = 0.04$, $R^2 = 0.80$, but not different from the four cues prediction, $t(3) = 0.61$, $p = 0.59$, $R^2 = 0.11$ (see Figure 8 for visual comparison of Mix path versus Combined Fit). Plotted as one to four cues, the decrease in thresholds for the Mix path was observed to obey a power function. Slopes for the Mix path were found to be significantly steeper than their respective PS predictions, $t(3) = 10.71$, $p = 0.002$, $R^2 = 0.97$ (see purple line vs purple dotted line in Figure 8).

Discussion

In this experiment, we set out to investigate how first- and second-order cues would interact on a common contour and if such a contour would be globally processed. In using the Mix path the number of cues on a contour could be increased gradually. Results obtained suggested that when a LD cue is added to preexisting second-order cues, global integration within the visual system uses the first-order information as well as the second-order information. This is in line with previous research that has combined luminance and contrast information on a common path and found that performance benefits cannot be explained by the integration of the second-order contrast information alone (Bell & Badcock, 2008), although there the second-order path contained no

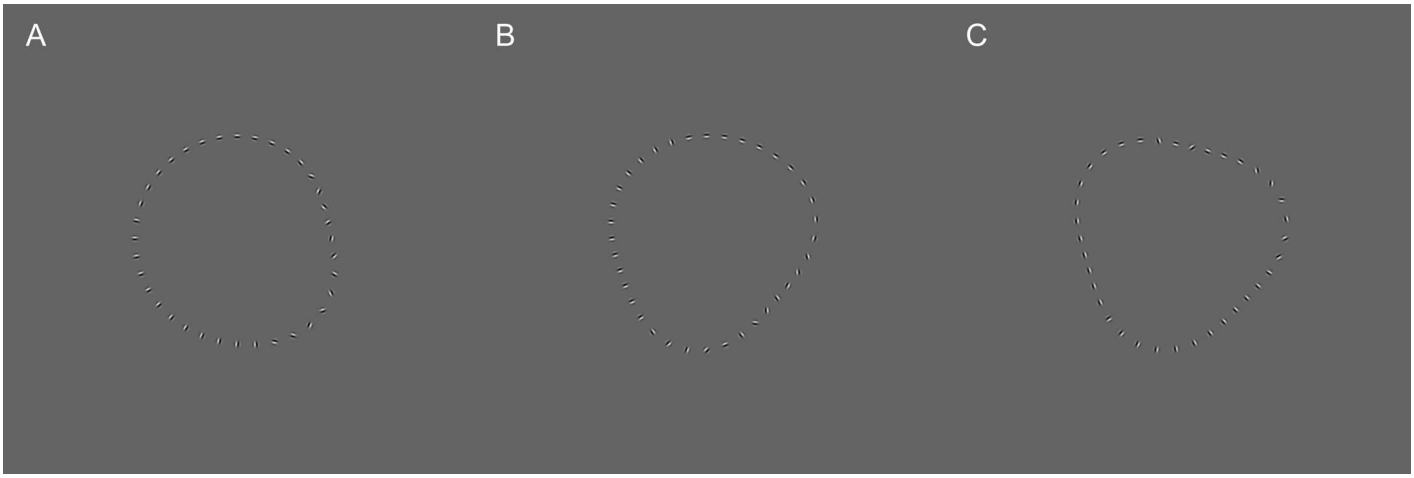

Figure 7. Examples of stimuli (Mix path) used in Experiment 2 with one to three CoMs (A–C, respectively). RF path, RFO path, and Rand path were combined on the same contour to create this stimulus. When modulation of the contour was present it always appeared in the Rand path portion for the first cycle (A), RFO path portion for the second cycle (B), and RF path portion for the third cycle (C). Stimuli are presented above threshold for illustration purposes.

oriented structure in the texture, unlike the current patterns. The suggestion that any performance benefit observed results from a probabilistic addition of cues can be rejected. The data suggests that when a usable LD cue is added to a preexisting second-order contour, the first- and second-order information contained within the LD cue is summed linearly. As number of cues increased, it was also observed that thresholds fell at a rate that exceeded a conventional estimate of PS, indicating that when LD and second-order information were presented on a path, the ensuing integration was a result of the linear pooling of both the first- and second-order information. While the previous study (Bell & Badcock, 2008) did demonstrate integration of a mixed luminance and contrast contour, the current experiment differed in that the sampled contour used was comprised of the same Gabor elements and as such did not have breaks between the sections (breaks were not at points of maximum curvature and hence did not interfere with global processes; Loffler et al., 2003). The current experiment shows that first- and second-order information is pooled linearly and not probabilistically.

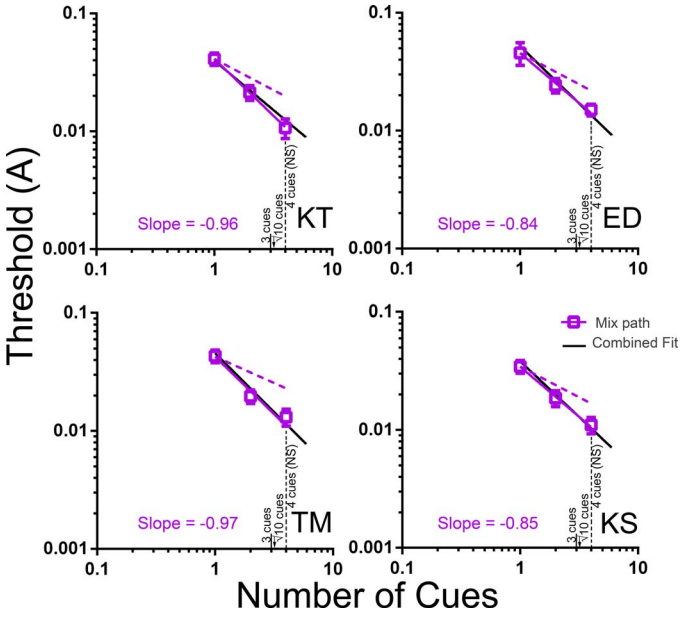

Figure 8. Thresholds for Mix path and Combined Fit plotted on logarithmic axes against number of cues with 95% CIs for each participant. Thresholds of the third CoM of the Mix path matched those for the prediction of four cues on the Combined Fit. The dashed purple line is the PS prediction for the Mix path. Slopes for Mix path were steeper than their PS prediction.

General discussion

Global integration has been shown to occur not only in RF patterns (Dickinson et al., 2010; Loffler et al., 2003; Tan et al., 2013) but also RF textures (Tan et al., 2015). As mentioned, the impression of the component elements flowing into closure (flowsure) was noted to be crucial for a modulated texture to be globally processed. It might be speculated that the reason integration occurs in textures that exhibit flowsure, but not otherwise, was that the orientation of a texture near a boundary might be more likely to be parallel to that boundary than perpendicular to the boundary. This might arise through truncation of lines at the boundary or foreshortening of lines perpendicular to a boundary when the extension of an object away from the boundary has a component in depth, as will very often be the case. Using the same reasoning, it might be

argued that if a path is defined by a texture perpendicular to the path then it is unlikely to define a boundary. Consequently, the first question addressed in the current study was whether a path with a texture perpendicular to the path might be disregarded as potentially describing the shape of an object. If this were the case, then we might expect a lack of integration of information around such a path. In Experiment 1A, however, it was demonstrated that textured contours whose component elements had orientations that were perpendicular to the path and therefore did not have the impression of flowsure (RFO path) could be globally integrated. Secondly, in Experiment 1B, it was shown that even when the textured contour did not possess any systematic variation in orientation information (Rand path), global integration of the contour could still be observed. This clearly demonstrated that textured contours were not governed by the same rules as modulated textures and that the textured contour did not take on the rules of the texture (for integration) since both the RFO path and the Rand path that had no component of flowsure were still globally processed. This led us to surmise that in a textured contour what was being pooled was not the local orientation information from the patches but rather the modulation information in the second-order path resulting from rectification of the Gabor patches. These results confirm that the mechanisms that support the integration of shape information in paths and texture differ. They also illustrate the distinction between the mechanisms that govern the salience of a path in noise and the mechanisms that analyze the shape of salient paths. A path of randomly oriented Gabors would be invisible in the context of a background of randomly oriented Gabor patches, so the demonstration of integration in a discrete path of randomly oriented patches strongly implies that the analysis of the shape of the path is performed solely using the second-order information. No integration is found for RFO textures and so the same must be true for the paths composed of patches oriented perpendicular to the path.

Stimuli resembling those used in this study (albeit with open contours) have been employed in previous studies, and have been referred to as snakes and ladders (Bex et al., 2001; Marotti et al., 2012). In these studies, snakes refer to open Gabor paths where the Gabor orientations are parallel to the path, while ladders refer to open Gabor paths where the Gabor orientations are perpendicular to the path. In the current study, the parallel for the snakes and ladders are the RF path and RFO path, respectively. The prior studies (Bex et al., 2001; Marotti et al., 2012) note that generally, snakes are more detectable than ladders when embedded in fields of Gabor noise. While the stimuli in the current study did not utilize contours embedded in noise elements, as shown in Figure 2, observers demonstrated lower thresholds for the RF path (the snake equivalent) in comparison to the RFO path (the ladder equivalent), suggesting a higher sensitivity for the RF path. This finding seems to be consistent with the prior studies as to the enhanced sensitivity for paths with orientations parallel to the path. It is worth noting here that while thresholds differ between RF and RFO paths, global processing—as indicated by the slope of the line describing the improvement in thresholds as more CoMs are added to the contour—remains unaffected.

More specifically, with the exception of one participant, it was noted that thresholds for the RF path (an LD contour) were approximately half those for the RFO path and Rand paths, supporting the arguments that these are both second-order contours. Experiment 2 then went on to examine the interaction of the first- and second-order cues in the analysis of shape. Findings from Experiment 2 suggest that the performance benefit observed was consistent with the RF path containing double the amount of signal, and given that it might be assumed that as the RF path comprised first- and second-order cues to shape, double the number of cues. Indeed when LD and second-order information was presented on a common contour, not only was integration observed as number of cues increased, it was demonstrated that the visual system was able to combine both first- and second-order information linearly. We propose that the process supporting global integration in shape channels is not order specific and can use both first- and second-order information equally.

The results of the series of experiments presented here confirm the distinction between the integration of modulation information in a path and within a texture. The shape information in a modulated path was integrated around the path even when the local orientation of the elements comprising the path was perpendicular to the path. This contrasts with the results from RF textures reported in Tan et al. (2015), which showed that integration of orientation information only occurred if the flow implied by the texture was predominantly concentric. A concentric flow might be expected adjacent to a bounding contour due to the truncation of radially oriented elements or the foreshortening of elements on a surface, which is not normally to the line of sight. On this point we conclude, therefore, that modulation of a predominantly concentric texture might provide information pertaining to the shape of the bounding contour of an object when the contour is not itself visible.

The conclusion that global processing was occurring arises from both the near −1 slopes, suggesting perfect integration of information, and the significantly steeper slopes than predicted by PS. It should

be noted that there are varying methods for the calculation of PS, and the one employed in this study is that recommended by Loffler et al. (2003) as outlined by Wilson (1980), which is derived from the Quick (1974) function. In instances where global integration fails, slopes obtained match a prediction for $-1/Q$ (Loffler et al., 2003), which suggests it might be a reasonable estimate to use. There have, however, been studies that criticize the use of the PS prediction generated in this manner, because it assumes that the threshold for each detector is sufficiently high that false-positive detection cannot be the result of random physiological noise—a high threshold theory assumption (Kingdom et al., 2015; Laming, 2013; Meese & Summers, 2012; Nachmias, 1981). Baldwin, Schmidtmann, Kingdom, and Hess (2015) have recently proposed that under signal detection theory, PS would yield slopes of −0.6 for their fixed-phase RF patterns. The authors also observe steeper functions from interleaving trials (than blocking trials), which is not unlike what we obtain for our random-phase stimuli. However, in comparison to both studies (Baldwin et al., 2015; Loffler et al., 2003), the slopes we obtain in the current study are steeper than their estimates of PS, and are sufficiently high that they approximate perfect integration. Therefore, it is safe to assume that global integration is occurring in the RF paths we have used. Furthermore, there is evidence that when a 2×2 forced choice task is run (with RF3s and RF6s), participants are able to identify which pattern is presented at the same modulation threshold required to detect deformation from circularity (Dickinson et al., 2013). This is consistent with different RF patterns being processed by separate information channels and provides further evidence that shape information in RF3 patterns is treated globally.

Keywords: shape, radial frequency pattern, global integration, first-order, second-order, texture, flowsure

Acknowledgments

This research was supported by Australian Research Council Grants DP1097003, DP0666206, and DP110104553 to DRB and a SIRF scholarship funded by the University of Western Australia to KWST.

Commercial relationships: none.
Corresponding authors: Ken W. S. Tan & David R. Badcock.
Email: tanw06@student.uwa.edu.au; david.badcock@uwa.edu.au.
Address: The University of Western Australia, School of Psychology, Crawley, WA, Australia.

References

Altmann, C. F., Bülthoff, H. H., & Kourtzi, Z. (2003). Perceptual organization of local elements into global shapes in the human visual cortex. *Current Biology*, *13*(4), 342–349.

Badcock, D. R., Almeida, R. A., & Dickinson, J. E. (2013). Detecting global form: Separate processes required for Glass and radial frequency patterns. *Frontiers in Computational Neuroscience*, *7*(53), 1–12.

Baldwin, A. S., Schmidtmann, G., Kingdom, F. A. A., & Hess, R. F. (2015). Rejecting probability summation for RF patterns, not so quick! *Journal of Vision*, *15*(12):1031, doi:10.1167/15.12.1031. [Abstract]

Bell, J., & Badcock, D. R. (2008). Luminance and contrast cues are integrated in global shape detection with contours. *Vision Research*, *48*, 2336–2344.

Bex, P. J., Simmers, A. J., & Dakin, S. C. (2001). Snakes and ladders: The role of temporal modulation in visual contour integration. *Vision Research*, *41*(27), 3775–3782.

Burr, D., & Ross, J. (2006). The effects of opposite-polarity dipoles on the detection of Glass patterns. *Vision Research*, *46*(6–7), 1139–1144.

Dickinson, J. E., Bell, J., & Badcock, D. R. (2013). Near their thresholds for detection, shapes are discriminated by the angular separation of their corners. *PLoS One*, *8*(5), 1–9.

Dickinson, J. E., Broderick, C., & Badcock, D. R. (2009). Selective attention contributes to global processing in vision. *Journal of Vision*, *9*(2):6, 1–8, doi:10.1167/9.2.6. [PubMed] [Article]

Dickinson, J. E., Cribb, S. J., Riddell, H., & Badcock, D. R. (2015). Tolerance for local and global differences in the integration of shape information. *Journal of Vision*, *15*(3):21, 1–24, doi:10.1167/15.3.21. [PubMed] [Article]

Dickinson, J. E., Han, L., Bell, J., & Badcock, D. R. (2010). Local motion effects on form in radial frequency patterns. *Journal of Vision*, *10*(3):20, 1–15, doi:10.1167/10.3.20. [PubMed] [Article]

Dickinson, J. E., McGinty, J., Webster, K. E., & Badcock, D. R. (2012). Further evidence that local cues to shape in RF patterns are integrated globally. *Journal of Vision*, *12*(12):16, 1–17, doi:10.1167/12.12.16. [PubMed] [Article]

Edwards, M., & Badcock, D. R. (1995). Global motion perception: No interaction between first and

second-order motion pathways. *Vision Research*, *35*(18), 2589–2602.

Field, D. J., Hayes, A., & Hess, R. F. (1993). Contour integration by the human visual system: Evidence for a local "association field." *Vision Research*, *33*(2), 173–193.

Graham, N. V. S., & Sutter, A. (1996). Effect of spatial scale and background luminance on the intensive and spatial nonlinearities in texture segregation. *Vision Research*, *36*(10), 1371–1390.

Habak, C., Wilkinson, F., & Wilson, H. R. (2009). Preservation of shape discrimination in aging. *Journal of Vision*, *9*(12):18, 1–8, doi:10.1167/9.12.18. [PubMed] [Article]

Habak, C., Wilkinson, F., Zakher, B., & Wilson, H. R. (2004). Curvature population coding for complex shapes in human vision. *Vision Research*, *44*, 2815–2823.

Kapadia, M. K., Westheimer, G., & Gilbert, C. D. (2000). Spatial distribution of contextual interactions in primary visual cortex and in visual perception. *Journal of Neurophysiology*, *84*(4), 2048–2062.

Kempgens, C., Loffler, G., & Orbach, H. S. (2013). Set-size effects for sampled shapes: Experiments and model. *Frontiers in Computational Neuroscience*, *7*, 1–18.

Kingdom, F. A. A., Baldwin, A. S., & Schmidtmann, G. (2015). Modeling probability and additive summation for detection across multiple mechanisms under assumptions of signal detection theory. *Journal of Vision*, *15*(5):1, 1–16, doi:10.1167/15.5.1. [PubMed] [Article]

Laming, D. (2013). Probability summation—A critique. *Journal of the Optical Society of America A*, *30*(3), 300–315.

Ledgeway, T., Hess, R. F., & Geisler, W. S. (2005). Grouping local orientation and direction signals to extract spatial contours: Empirical tests of "association field" models of contour integration. *Vision Research*, *45*(19), 2511–2522.

Li, W., & Gilbert, C. D. (2002). Global contour saliency and local colinera interactions. *Journal of Neurophysiology*, *88*(5), 2846–2856.

Loffler, G. (2008). Perception of contours and shapes: Low and intermediate stage mechanisms. *Vision Research*, *48*, 2106–2127.

Loffler, G. (2015). Probing intermediate stages of shape processing. *Journal of Vision*, *15*(7):1, 1–19, doi:10.1167/15.7.1. [PubMed] [Article]

Loffler, G., Wilson, H. R., & Wilkinson, F. (2003). Local and global contributions to shape discrimination. *Vision Research*, *43*(5), 519–530.

Marotti, R. B., Pavan, A., & Cascoa, C. (2012). The integration of straight contours (snakes and ladders): The role of spatial arrangement, spatial frequency and spatial phase. *Vision Research*, *71*, 44–52.

Meese, T. S., & Summers, R. J. (2012). Theory and data for area summation of contrast with and without uncertainty: Evidence for noisy energy model. *Journal of Vision*, *12*(11):9, 1–28, doi:10.1167/12.11.9. [PubMed] [Article]

Motoyoshi, I., & Kingdom, F. A. A. (2010). The role of co-circularity of local elements in texture perception. *Journal of Vision*, *10*(1):3, 1–8, doi:10.1167/10.1.3. [PubMed] [Article]

Nachmias, J. (1981). On the psychometric function for contrast detection. *Vision Research*, *21*(2), 215–223.

Nygård, G. E., Sassi, M., & Wagemans, J. (2011). The influence of orientation and contrast flicker on contour saliency of outlines of everyday objects. *Vision Research*, *51*(1), 65–73.

Poirier, F. J. A. M., & Wilson, H. R. (2006). A biologically plausible model of human radial frequency perception. *Vision Research*, *46*(15), 2443–2455.

Quick, R. F. (1974). A vector-magnitude model of contrast detection. *Biological Cybernetics*, *16*(2), 65–67.

Schmidtmann, G., Kennedy, G. J., Orbach, H. S., & Loffler, G. (2012). Non-linear global pooling in the discrimination of circular and non-circular shapes. *Vision Research*, *62*, 44–56.

Tan, K. W. S., Bowden, V. K., Dickinson, J. E., & Badcock, D. R. (2015). Modulated textures with shape structures implied by a closed flow are processed globally. *Journal of Vision*, *15*(3):17, 1–18, doi:10.1167/15.3.17. [PubMed] [Article]

Tan, K. W. S., Dickinson, J. E., & Badcock, D. R. (2013). Detecting shape change: Characterizing the interaction between texture-defined and contour-defined borders. *Journal of Vision*, *13*(14):2, 1–16, doi:10.1167/13.14.2. [PubMed] [Article]

Tversky, T., Geisler, W. S., & Perry, J. S. (2004). Contour grouping: Closure effects are explained by good continuation and proximity. *Vision Research*, *44*(24), 2769–2777.

Tyler, C. W., & Chen, C.-C. (2000). Signal detection theory in the 2AFC paradigm: Attention, channel uncertainty and probability summation. *Vision Research*, *40*, 3121–3144.

Wilder, J., Feldman, J., & Singh, M. (2016). The role of

shape complexity in the detection of closed contours. *Vision Research, 126*, 220–231, doi:10.1016/j.visres.2015.10.011.

Wilkinson, F., Wilson, H. R., & Habak, C. (1998). Detection and recognition of radial frequency patterns. *Vision Research*, *38*(22), 3555–3568.

Wilson, H. R. (1980). A transducer function for threshold and suprathreshold human vision. *Biological Cybernetics*, *38*(3), 171–178.

Wilson, H. R., Ferrera, V. P., & Yo, C. (1992). A psychophysically motivated model for two-dimensional motion perception. *Visual Neuroscience*, *9*(1), 79–97.

Wilson, H. R., & Wilkinson, F. (2015). From orientations to objects: Configural processing in the ventral stream. *Journal of Vision*, *15*(7):4, 1–10, doi:10.1167/15.7.4. [PubMed] [Article]